Optical Subnet Concepts for the Deep Space Network

K. Shaik and D. Wonica
Communications Systems Research Section

M. Wilhelm
Telecommunications Systems Section

This article describes potential enhancements to the Deep Space Network, based on a subnet of receiving stations that will utilize optical communications technology in the post-2010 era. Two optical subnet concepts are presented that provide full line-of-sight coverage of the ecliptic, 24 hours a day, with high weather availability. The technical characteristics of the optical station and the user terminal are presented, as well as the effects of cloud cover, transmittance through the atmosphere, and background noise during daytime or nighttime operation on the communications link. In addition, this article identifies candidate geographic sites for the two network concepts and includes a link design for a hypothetical Pluto mission in 2015.

I. Introduction

Communications systems are inherently capable of operating at higher antenna gain and modulation bandwidth as carrier frequency increases. Optical frequencies (approximately 10^{14} Hz) are several orders of magnitude higher than the operating carrier frequencies of the conventional RF communication systems (approximately 10^{10} Hz) in use today.

The promise of the large antenna gain and modulation bandwidth that become available at optical frequencies is the basic reason for the interest in the development of optical communication systems.

Optical systems also promise smaller size and mass and lower power consumption as compared to RF systems with similar performance characteristics. For planetary space missions, the advantage of reduced size, mass, and power requirements will allow more room for science instrumentation aboard a spacecraft.

The optical subnet concepts for the DSN reported in this article were developed, and their telemetry performance was estimated, for the Ground Based Advanced Technology Study (GBATS). The GBATS work was performed in conjunction with Deep Space Relay Satellite System (DSRSS) study contracts,[1,2] and its purpose was to initiate exploration of Earth-based alternatives to the

[1] JPL Contract 958733 with TRW, Jet Propulsion Laboratory, Pasadena, California, March 28, 1990.

[2] JPL Contract 958734 with STEL, Jet Propulsion Laboratory, Pasadena, California, March 28, 1990.

DSRSS that would allow significantly higher telemetry rates for future NASA deep-space missions.

The GBATS study of optical subnets draws on previous design studies of the Deep Space Optical Reception Antenna (DSORA) [1] and on a weather model [2,3] of ground-based laser communications. The GBATS study also makes use of work accomplished by TRW, one of the contractors working on the DSRSS study, for the user-terminal design concept.[3] The emphasis of the work was on telemetry support. It is anticipated that future work on the optical subnets will include uplink command, navigation, and optical science.

This article describes initial concept designs for an optical subnet to augment the DSN. In Section II, a description of the ground optical terminal, which forms the basis of the optical subnet, and a description of the user-spacecraft terminal are provided. An overview of the optical subnet concepts is provided in Section III. The propagation and weather models are developed in Section IV to provide a basis for the calculation of network availability and coverage. No specific planetary missions are considered for the optical subnets discussed here, though a hypothetical Pluto mission in 2015 is used as an illustration (see Section IV). Accordingly, the future considerations of mission sets, operational issues, enhancement of a ground station's capabilities, etc., may profoundly affect the performance, configuration, and operation of an optical subnet.

II. Ground and Spacecraft Optical Terminals

A. Ground Optical Terminal

Each optical station operates in the direct detection mode at optical wavelengths between 500 and 2000 nm. All calculations in this study were made using 532 nm as the operating wavelength. The telescope consists of a 10-m, non-diffraction-limited, segmented primary mirror and a secondary mirror, in a Cassegrain configuration, as shown in Fig. 1. The telescope is mounted on azimuth–elevation gimbals and is housed in an environmental enclosure (dome). The receiver subsystem includes the beam-reducer optics, steering mirror, tracking detector, and the communications detector. Facilities for data processing, ground communications, logistics, and security, as well as office space and other uses, are identified in this section for completeness, but are not examined in detail in this article.

[3] TRW briefing, "Deep Space Relay Satellite System Study," Quarterly Progress Review, presented to JPL on February 25, 1993.

The optical terminal as described in this section provides the basic building block of the optical subnets. The performance of the optical subnets, calculated in the following sections of the article, was based on the capabilities of a single ground station. The following assumptions and guidelines were used to arrive at a definition of the ground optical terminal:

(1) A 10-m-diameter primary mirror.

(2) Telemetry reception under both daytime and nighttime conditions.

(3) Telemetry reception within 10 deg of the Sun.

(4) Operating wavelength of 532 nm.

(5) Tracking and slew rates compatible with deep-space probes.

(6) Acquisition of a user signal within 20 minutes at an elevation angle of about 15 deg under all operating conditions.

(7) A 2-mrad field of view (FOV) for the Cassegrain receiver telescope with a coarse pointing accuracy of 0.2 mrad.

(8) A 0.1-mrad FOV for the communications detector (this matches the blur diameter of the telescope).

(9) A fine pointing mechanism with an accuracy of 0.01 mrad.

(10) Station operation at high altitudes to reduce the impact of the atmosphere (up to 4.2 km).

(11) Uplink transmitter, command, emergency command, and navigation requirements were not considered at this time.

B. Block Diagram of the Optical Ground Station

Figure 2 describes the flow of information and control signals for the receive system of the optical station. The telescope with a 10-m fast primary collects optical energy and delivers it to the Cassegrain focus. The wide-FOV sensor provides calibration, removes systematic telescope-mount error, and helps in the acquisition of the user spacecraft within the telescope coarse FOV. From here the incoming beam is further reduced, is controlled, and is delivered to the communications detector. The communications detector demodulates the optical signal, and the resultant data stream is fed to the signal processor for bit/frame synchronization, decoding, error checking, etc. From the signal processor, the data are sent to the Ground Communications Facility (GCF) for transmission to the Network Operations Control Center (NOCC) in real time.

Raw or processed data are also stored in the archival subsystem for playback in case of GCF outage. The executive controller manages station activities automatically or manually through the command console, communicates with the outside world through the ground communications facility, and receives inputs from and sends commands to slave computers which include the pointing controller, the tracking controller, the figure controller, the signal processor, and the facility controller.

C. Ground Terminal Architecture

The system breakdown for the optical station is shown in Fig. 3. Note that subsystems other than the optical terminal are mentioned here for completeness and are not discussed any further. Additionally, the subsystems related to an optical uplink transmitter are not considered at this time.

1. Optical Terminal. An optical terminal consists of the following subsystems:

a. Telescope and Optics. The telescope subsystem provides an aperture to collect necessary photons for direct detection of incoming signals. The telescope employs a 10-m segmented primary mirror. There are 60 hexagonal segments, arranged in four rings, with each segment about 1.1 m in size (see Fig. 1). Other elements of the receiver telescope include a secondary-mirror assembly, a truss support structure, appropriate baffles to avoid the Sun, and other optics as needed. Each of the mirror assemblies includes mounts and the necessary actuators and baffles.

Table 1 provides a representative prescription for a Ritchey–Chretien Cassegrain telescope. The focal ratio for the 10-m segmented and hyperbolic primary is 0.5. The secondary mirror is 4.5 m from the primary mirror and is 1 m in size. The Cassegrain focus, where the optical communication instrument will be placed, is 3.25 m behind the primary. The image size at the Cassegrain focus for the usable diametric FOV (2 mrad) is about 16 cm.

b. Receiver Subsystem. The receiver subsystem consists of the optical communications instrument (OCI), which includes the receive beam-control optics (the beam-reducer optics, steering mirror, spectral filter, etc.), the tracking detector, and the communication detector. Fine pointing and tracking of the spacecraft are achieved by the OCI. Once coarse pointing is established by the acquisition, pointing, and tracking (APT) assembly, the OCI uses the communication signal as a beacon to aid in the fine acquisition, pointing, and tracking process. The communication detector begins telemetry reception and transfers it to the signal-processing subsystem once tracking has been established.

Figure 4 shows a conceptual drawing of the OCI with its optics, spatial and spectral filters, steering mirror, and detectors. The received beam at the Cassegrain focus is corrected by a field corrector, spatially filtered by the field lens, and reduced and collimated by the reducer optics. The beam is spectrally filtered and steered by a two-axis steering mirror for fine pointing. A tracking detector is used to acquire, track, and center the received beam on the communications detector. The diametric FOV of the communications detector is restricted to 0.1 mrad.

c. Acquisition, Pointing, and Tracking. The APT assembly uses computer controlled azimuth–elevation gimbals. The telescope is mounted on the gimbals, and this mounting provides coarse pointing to and tracking of the user spacecraft. Initial coarse pointing coordinates, which will be used to bring the spacecraft within the telescope FOV, will be provided by the DSN. The network configurations studied here allow roughly 20 minutes to acquire the spacecraft and establish tracking.

Table 2 provides estimates of the pointing and tracking requirements. The coarse pointing requirement (0.2 mrad) is chosen to be an order of magnitude less than the useful Cassegrain FOV. The fine pointing requirement (0.01 mrad) is an order of magnitude less than the communication detector's FOV. The tracking rate is consistent with sidereal tracking requirements for deep space spacecraft. If the ability to track highly elliptical orbits (HEO's) is considered necessary, the tracking and slew rates must be revised upward as needed.

d. Environmental Housing. The environmental housing will consist of a protective dome over the telescope structure. Figure 5(a) shows a conceptual diagram for the dome when the dome is closed. It is similar to the dome built for the Air Force Starfire Optical Range's 3.5-m facility in New Mexico. The dome protects the telescope from catastrophic failure due to severe weather and protects optical coatings on the primary and the secondary from premature degradation. Figure 5(b) shows the telescope fully exposed under normal operating conditions when the dome is folded down to the pier.

D. Configuration of the User-Spacecraft Terminal

The user spacecraft terminal configuration used in this article is based on a TRW concept for a future optical

terminal.[4] A block diagram for the user terminal is shown in Fig. 6. The telemetry data are encoded via a pulse position modulation (PPM) scheme, and provided to the modulator drive electronics. A modulated diode-pumped neodymium-doped: yttrium aluminum garnet (Nd:YAG) laser beam travels through a frequency doubler, a beam expander, a two-axis point-ahead mirror, a two-axis fine-steering mirror, and then exits from the telescope. The transmitter employs a 0.75-m telescope with no obscuration. The transmit wavelength is 532 nm. A small fraction of the transmit laser energy is directed toward acquisition and tracking electro-optics that use a beam splitter and a corner cube to determine the point ahead.

Table 3 shows a list of important transmitter parameters and the values used to estimate telemetry capability. See Appendix A for further details on communications link calculations.

III. Subnet Overview

A. Operations Concept

Like the current DSN, link geometry drives the major characteristics of the optical subnet. DSN user spacecraft with interplanetary trajectories will require multiple stations located about the equatorial region to provide continuous telemetry support to any point near the ecliptic plane. As the Earth rotates, continuous telemetry coverage is provided to any given user spacecraft via a hand-off strategy between the stations. As each station comes within the line of sight (LOS) of a user and good link geometry is established, telemetry reception begins. As the Earth continues to rotate and the user passes into the LOS of the next optical station, a hand-off occurs. Initial acquisition and tracking of a user spacecraft begin with the reception of the user ephemeris data provided by the NOCC. The user ephemeris provides coarse pointing information for acquiring the user transmit signal within the FOV of the telescope. Once coarse pointing is established by identifying the received beam on the acquisition and tracking detector, the receiver subsystem uses a fast steering mirror for fine pointing and centering of the signal beam on the communications detector. User spacecraft tracking is maintained throughout the pass by the combined action of the coarse pointing mechanism of the telescope and the fine steering mirror. The acquisition sequence followed by telemetry reception is repeated with down-line stations for the duration of the user spacecraft's need.

User spacecraft pointing is established by detection of an uplink beacon, detection of the crescent Earth, or detection of the Sun with the point ahead off-set to the Earth (user spacecraft pointing is not part of GBATS). Coarse pointing is provided by the spacecraft attitude-control system from data provided by an onboard star tracker. Once the target (Earth) is acquired within the FOV of the user-spacecraft telescope, a fast steering mirror fine points and centers the target on a charge-coupled device (CCD) array. Data transmission begins once user pointing is established.

Based upon a 30-AU Pluto mission, and a 0.75-m user aperture, the footprint of the beam transmitted by the user terminal is smaller than the Earth's diameter; therefore, it is necessary to point the beam to the designated receiving station accurately. This can be accomplished without difficulty since the pointing bias and jitter errors, as shown in the earlier section on the user-terminal design, are much smaller than the signal beam diameter. A station is designated to receive telemetry when (1) it is within the LOS of the user terminal and (2) it has cloud-free weather. The need to predict weather availability for some subnet configurations is addressed in appropriate sections below. (Weather availability is a measure of station outage due to weather effects such as clouds, rain, and dense fog.)

The baseline for this study provides for one receive aperture per geographic location. This places some restrictions on simultaneous support of multiple missions. For example, user spacecraft with simultaneous-coverage requirements must be located nominally 180 deg apart.

B. Subnet Configurations

The presence of opaque clouds generally limits the availability of a single ground station for optical communications to less than 70 percent. This problem can be handled by employing spatial diversity.

There are two fundamentally different methods to provide the necessary spatial diversity to improve network weather availability for optical communications. The two concepts use different strategies in the location of optical stations to provide station diversity. These two approaches are referred to as the clustered optical subnet (COS) concept and the linearly dispersed optical subnet (LDOS) concept. In this article, two specific configurations, based on the COS and the LDOS concepts, were developed in detail. They were a COS network with nine stations and an LDOS network with six stations. Both configurations were developed based upon site-specific weather statistics, site surveys (accomplished by literature searches), coverage analysis, and projected telemetry performance. While

[4] Ibid.

they use the same 10-m optical station and the same basic operations concept, each subnet offers unique advantages and disadvantages. Each subnet is designed to provide high weather availability. A detailed characterization of the two concepts and the reasons for selecting the number of stations in each case are provided in Section IV.

It is assumed that each station will require less than 20 minutes to acquire, track, and lock onto the incoming optical beam for both the LDOS and the COS concepts.

Figure 7(a) depicts network geometry for an LDOS showing three ground stations, and Fig. 7(b) depicts geometry for a COS network showing two of the clusters, each with three stations. Telemetry received by the available station for each subnet concept is demodulated and sent to the station data processing subsystem for one of three purposes: processing and formatting, storage in the archival subsystem, or for transmission in raw form to JPL's NOCC for distribution to end users. The stations are connected to the existing DSN infrastructure via the GCF.

IV. Performance Analysis

To develop optical network configurations that meet certain performance goals, several analyses were performed to identify a preferred approach. These efforts included the development of a propagation model, a weather model, an ideal-coverage model for the COS and the LDOS concepts, and availability assessments for various network configurations. For illustrative purposes, two network configurations, one from among the COS concepts and one from among the LDOS concepts, were selected for detailed study. For these two configurations, an LDOS with six stations and a COS with three clusters of three stations (COS 3 × 3), a coverage analysis was made for ideal conditions, as was a telemetry performance projection for a Pluto mission in the year 2015.

A. Propagation Model

Earth's atmosphere has a dominating impact on the propagation model for ground-based optical communications. Propagation loss and sky background radiance are two significant factors. Propagation loss, that is, loss due to transmission through the atmosphere, can be predicted using semiempirical models under various operating conditions. The problem of opaque cloud cover is studied in Section IV.B, where a weather model is produced.

The U.S. Standard Atmosphere 1976 model was used in this study to evaluate the effects of station altitude, meteorological range (i.e., visibility), and zenith angle. Section IV.A.1 shows that the impact of using atmospheric models other than the U.S. Standard Atmosphere 1976 is very small.

It is also important to study the impact of sky background noise on optical communications, especially the impact during daytime operations. This is addressed in Section IV.A.5. The results are used to develop average telemetry rates for daytime operations in Section IV.F.

1. Atmospheric Transmittance Model. LOWTRAN7, a transmittance model developed by the Air Force Geophysics Laboratory (AFGL) for visible and infrared wavelengths, was used to calculate propagation effects on wavelengths of interest, including 532 nm. The results of using the U.S. Standard Atmosphere 1976, mid-latitude winter, and mid-latitude summer atmospheric models on the transmittance, which was supplied by LOWTRAN7, are shown in Fig. 8(a). The curves shown for all the models assume the presence of high cirrus clouds, a 2.3-km altitude for the ground station, a 17-km meteorological range (visibility), and a zenith path through the atmosphere. Since the atmospheric transmittance models do not differ significantly from each other, the U.S. Standard Atmosphere 1976 model was used to calculate nominal spectral transmittance under all operating conditions.

2. Spectral Transmittance Versus Altitude. Figure 8(b) shows the transmittance for selected altitudes as predicted by LOWTRAN7. In the ideal-coverage model, the station altitude (2.3 km) of the Table Mountain Facility (TMF) was used as the baseline for the optical stations. Altitudes for the actual locations were used once specific LDOS and COS configurations were developed.

3. Spectral Transmittance Versus Meteorological Range. Varying meteorological range (visibility) will have an impact on the transmittance of the optical beam. Figure 8(c) shows the spectral transmittance for selected visibilities for wavelengths between 0.4 and 2.0 μm. A meteorological range of 17 km (defined as clear) was used as the basis for all calculations in this article.

4. Spectral Transmittance Versus Zenith Angle. The most dominant factor influencing the transmittance of the optical beam through the atmosphere is the operational zenith angle during telemetry reception. Figure 8(d) is a LOWTRAN7 plot of spectral transmittance for selected zenith angles for wavelengths between 0.4 and 2.0 μm. At a 70-deg zenith angle, the air mass through which the signal must propagate is about three times larger than the air mass at zenith. This is equivalent to about 17 dB of loss. In this article, the telemetry reception of the

optical station down to a zenith angle of 70 deg is included in the coverage analysis and link calculations.

5. Optical Background. Optical communications system performance in terms of data rate varies significantly between night and day. For a ground-based receiver, the sky radiance is a major source of optical noise, especially for daytime operation. This information was factored in when data volume over a 24-hour period was calculated for the GBATS work.

a. Nighttime. The sky brightness at night is about 50 nW/(m^2·nm·sr). This brightness is equivalent to a star of visual magnitude of 21.25 per square arcsec [4].

b. Daytime. Figure 9 shows sky radiance as a function of solar elongation. Sky radiance decreases by an order of magnitude for solar elongation (Sun–Earth–spacecraft angle) of 180 deg from a high of about 0.6 W/(m^2·nm·sr) when one is looking about 10 deg from the Sun. The graph is derived from LOWTRAN7 calculations for normal weather (17-km visibility) for a TMF-like receiver site. An average daytime data rate was calculated using six representative daytime sky radiances, specifically at 10-, 40-, 70-, 100-, 130-, and 160-deg solar elongation.

B. Weather Model and Availability Analysis

Besides geometry, the largest driver in terms of network performance is weather availability. With optical communications, the effects of weather on station availability are significantly more severe than they are at microwave frequencies. Unlike microwave frequencies, practically no communications can take place when the propagation path for an optical link is blocked by clouds. In this article, a weather model developed by Shaik [2] was used to model weather effects on link availability for optical stations in spatially independent weather cells. A total network availability of 90 percent was chosen as the performance goal.

1. Weather Model. For potential optical station sites, rough estimates of pertinent weather statistics can be obtained from existing sources, which include weather satellites. Figure 10 shows a contour diagram for the probability of a clear sky over the United States obtained from two years of GOES satellite data [5]. As can be seen, the probability of cloud-free skies over Southern California is about 66 percent. This means that 34 percent of the time, this area has partial to full cloud cover. To provide high weather availability (approximately 90 percent) requires that multiple stations be within the line of sight of the user spacecraft but located in different uncorrelated cells.

Based upon empirical information obtained from the AFGL, the cloud-system correlation coefficient between sites was expressed as[5]

$$\rho = \exp\left[-\Delta x^2/2\sigma^2\right] \tag{1}$$

where Δx is the distance between sites and $\sigma = 50$ km. This empirical result is then used to obtain the extent of cloud-system correlation for any two sites. An intersite distance of at least 3–4 σ, (or about 150–200 km) for $\rho \leq 0.01$ is found adequate to ensure spatially independent weather cells.

Given ground stations in spatially independent weather cells, a parametric weather model [2] can be used to compute link availability statistics. The model may be used to predict the joint probability (the percentage of time) that the extinction loss due to the atmosphere is less than some threshold for at least one of the ground stations. We define $\omega_n(L)$ as the cumulative distribution function (CDF)—that is, as the fraction of time when the propagation loss due to the atmosphere is less than or equal to L dB for at least one of the n sites with a line of sight to the user spacecraft. The weather availability can then be expressed as the CDF

$$\omega_n(L) = 1 - \{q \exp[-0.23b(L - L_0)]\}^n; \quad (L \geq L_0) \tag{2}$$

where L_0 is the acceptable loss through the atmosphere in dB and defines the operational telemetry line for the optical subnet. The minimum loss through the atmosphere is given by $\eta_a \sec(\zeta)$ in dB, where ζ is the zenith angle and η_a represents a site-altitude-dependent empirically derived propagation loss through the atmosphere under normal clear conditions. Since $\eta_a \sec(\zeta)$ estimates the minimum possible loss through the atmosphere, $L_0 \geq \eta_a \sec(\zeta)$. Parameter b is a site-dependent parameter and is derived empirically to model the CDF curve [2]. In this study, $b = 0.11$ and is derived from the assumption that $\omega_1(L = 30) = 0.8$ at zenith.[6] The equation assumes that the probability of cloudy skies, q, is the same for all sites, but it can easily be extended to site dependent q.

Equation (2) provides a simple model to compute the weather availability of an optical subnet. For example, under normal weather conditions for the Table Mountain

[5] K. Shaik, "Spatial Correlation of Cloud Systems," JPL Interoffice Memorandum 331-88.6-564 (internal document), Jet Propulsion Laboratory, Pasadena, California, October 7, 1988.

[6] The probability of opaque clouds occurring in the Southwestern United States is less than 20 percent [2].

Facility, the minimum propagation loss at $\zeta = 60$ deg is -4.7 dB. Choosing this as the acceptable propagation loss, $L_0 = -4.7$ dB, and with $q = 0.34$ at TMF, the availability of a single site for $L = L_0$ is found to be $\omega_1(L_0) = 0.66$. If there are three such independent and identical sites in a subnet within the LOS of the user spacecraft, then from Eq. (2), the subnet availability is found to be $\omega_3(L_0) = 0.96$.

2. Weather Availability. As previously mentioned, weather availability is a measure of station outage due to weather effects such as clouds, rain, and dense fog. Individual sites for an optical subnet were chosen for their good cloud-free statistics, and are located far enough apart, as determined by Eq. (1), to ensure independent weather from station to station. The availability of a single station is expected to be at least 66 percent. The availability of a given network configuration is discussed in Section IV.D.

C. Coverage Analysis

LOS coverage (or, more simply, coverage) is defined as the percent of time during a 24-hour period when an unobstructed path, excluding weather conditions, exists between one or more stations on Earth and the user spacecraft. The performance goal for all networks is to provide 100 percent coverage.

A ground-based network consists of Earth stations strategically placed around the globe to provide full coverage, 24 hours a day. Ideally, only two stations located near the equator and placed exactly 180 deg apart would be required to provide full coverage. However, the number of stations quickly increases due to the constraint of the minimum operational elevation angle of 15 or 30 deg, the fact that the stations cannot always be placed at the equator, and the need to have more than one station in the spacecraft LOS to provide high weather availability. Specific network configurations and the coverage they provide are presented in the following paragraphs.

D. Network Analysis

The most promising network concepts which provide high weather availability and full coverage of the ecliptic were introduced in Section III.B earlier. In this section, subnet concepts are described in greater detail under idealized conditions to provide a rationale for the selection of promising configurations. The selected configurations, an LDOS with six stations and a COS configuration with nine stations, were then studied under realistic conditions with reference to a Pluto mission in 2015. The coverage curves and the telemetry rates are derived using actual site parameters, including longitude, latitude, altitude, and cloud-cover statistics, obtained from satellite data or in situ observations, and compared to the results obtained under ideal conditions.

1. LDOS Analysis. In this study, LDOS configurations were designed with six to eight ground stations spaced roughly equidistant from each other and placed around the globe near the equatorial region. An LDOS with five stations was not considered since the availability of this configuration is considerably below 90 percent (the percent required by the GBATS guidelines), and because the optical subnet would need to operate at very low elevation angles for a large fraction of the time.

Since the characteristic cloud systems calculated according to Eq. (1) are of the order of a few hundred kilometers in size, which is much smaller than the interstation distance, the adjacent stations will lie in different climatic regions and thus have uncorrelated cloud-cover statistics. Once specific sites were chosen, single as well as joint cloud-cover statistics for two or more consecutive sites were evaluated and used to predict link availability.

The probability of link outage for the LDOS configuration is low because (a) several stations are within the LOS of the user spacecraft, and (b) the stations lie in different climatic zones and hence their weather patterns are uncorrelated. Since the receiving sites are far apart, data with high spatial resolution on cloud-cover statistics are not needed. Existing data with a resolution of about 100 km are sufficient. However, further site surveys are needed to provide weather data with high temporal resolution. The weather data with high temporal resolution are needed to compute and predict short-term outage statistics accurately. Weather data with hourly or better temporal resolution will probably be needed to finalize site selection.

The distance between the receiving stations in the LDOS concept is very large; therefore, the full benefit of using optical wavelengths can be realized only when the user spacecraft points accurately to the designated receiving station in the subnet. Since the spacecraft can be 4–5 light hours from the Earth for some planetary missions, the weather availability of the subnet has to be predicted several hours in advance to designate the receiving station, and the location of the designated station must be uplinked to the user spacecraft terminal for pointing purposes.

a. LDOS With Six Ground Stations. The LDOS which consists of six optical stations located approximately 60 deg apart in longitude about the equatorial region is

shown in Fig. 11. Each optical station is located in a different climatic region (approximately 7000 km apart), and thus they have statistically uncorrelated cloud cover.

Figure 12 shows ideal coverage curves for six stations 60 deg apart in longitude. To calculate propagation loss, the model assumes that all station sites have normal visibility (17 km) and are as high as the Table Mountain Facility (2.3 km). It is also assumed that each site has cloud-free days at least 66 percent of the time (i.e., $q = 0.34$). For this configuration, only two stations will have LOS coverage of the spacecraft at all times when the telemetry line (acceptable zenith angle loss through the atmosphere) is consistent with a 60-deg zenith angle. The availability for this optical subnet is calculated to be $\omega_2(L_0) = 0.88$. The availability of the subnet can be increased to about 92 percent if a telemetry line consistent with a 75-deg zenith angle can be used.

Consider the situation when station 3 is receiving from a spacecraft on an equatorial path. The natural point to hand-off telemetry to station 4 is when zenith angle $\zeta_3 = \zeta_4 = 30$ deg (the subscript refers to the station number). Note that while ζ_3 is increasing, ζ_4 is decreasing. As calculated from the weather model described above, about 12 percent of the time, station 4 will be unavailable due to weather. In this case, station 3 continues to receive up to the point when $\zeta_3 = 60$ deg, at which point station 5 is activated at $\zeta_5 = 60$ deg. For this configuration, the telemetry line is placed at $\zeta = 60$ deg. The necessary trade-offs to optimize the position of the telemetry line have not been made. This leaves about one hour for acquisition and overlap between stations, as the stations are required to operate down to $\zeta = 75$ deg in zenith.

Table 4(a) provides a list of possible geographical sites for this LDOS configuration as an example. Appendix B describes the guidelines and the procedures used to select geographical sites in Table 4(a) and the following site tables. Weather statistics for all locations, except for the Hawaii and Chile sites, were obtained using satellite data [6] and are shown in Table 4(a). The data used for Hawaii and Cerro Pachan in Chile were based upon in situ observations [7]. Table B-1 in Appendix B lists possible additional sites.

Using specific sites given in Table 4(a) and assuming a hypothetical mission to Pluto in 2015 for illustrative purposes, a set of coverage curves was derived for a realistic LDOS with six stations. Figure 13 shows the coverage curves when data on actual geographical sites are used for the Pluto mission. The site-specific information used to obtain these curves includes altitude, longitude, and latitude, as well as Pluto's trajectory across the sky. Note that Pluto does not pass through the zenith for any of the sites. As can be seen in the figure, coverage will last from 2.5 to 4 hours, depending on the specific latitude of the optical station. For example, at the site in Siding Spring Mt., Australia, a telemetry pass will last approximately 4 hours.

A close examination of Fig. 13 shows that the telemetry line has been placed a little lower compared to Fig. 12. The acceptable atmospheric loss for the realistic Pluto mission is about −6.2 dB, instead of −4.7 dB for the ideal case, and corresponds to a 70-deg zenith angle rather than the 60-deg angle used in the ideal case. The introduction of actual geographical parameters has reduced the network availability for an LDOS with 6 stations from 88 percent for the ideal case to 81 percent. Also note that the acquisition time is about 20 minutes for the Pluto mission case instead of 1 hour for the ideal case.

b. LDOS With Seven Ground Stations. The interstation distance in this case will be roughly 51 deg in longitude (approximately 6000 km). Here, 35 percent of the time, three stations will be 30 or more deg above the horizon. The rest of the time, only two stations will be available. Availability for this configuration, when two or three stations are above 30 deg in elevation, is calculated to be $\omega_{2/3}(L_0) = 0.65\omega_2(L_0) + 0.35\omega_3(L_0) = 0.91$. The telemetry line for this configuration is at a 60-deg zenith angle. Table 4(b) provides a list of possible geographical sites. Table B-1 in Appendix B lists possible additional sites.

c. LDOS With Eight Ground Stations. The interstation distance for this configuration will be roughly 45 deg in longitude (approximately 5000 km). This configuration will ensure that three stations are 30 or more deg above the horizon about 66 percent of the time in a 24-hour period. An LDOS with 8 stations will provide 94 percent availability. The telemetry line is at a 60-deg zenith angle as before, providing considerably long overlap between stations. Table 4(c) shows a list of possible geographical sites for this configuration.

2. Analysis for the Clustered Optical Subnet. For geopolitical or operational reasons, the stations of an optical subnet may be required to be located within three or four locations around the globe that were chosen for their optimally cloud-free skies. In this concept, a cluster of three stations no more than a few hundred kilometers apart is envisioned for each of the selected regions. This distance is necessary to ensure that each station is located in a unique weather cell. For a major portion of the time, the spacecraft points to only one of these clusters; the

spacecraft hands over the signal beam to the next cluster as the spacecraft rises sufficiently above the horizon. Since the intracluster distance between stations is of the order of a few hundred kilometers, cloud-cover data with much finer spatial resolution (a few tens of kilometers) than for the LDOS configuration are required. In addition, the requirements for obtaining site-specific cloud-cover data with sufficient temporal resolution, which were discussed previously, apply here as well.

An advantage of the COS concept over the LDOS is that there is no need to predict weather availability several hours in advance. All stations within a cluster monitor the user-spacecraft's transmitted beam jointly with little pointing loss. Additionally, there is no need to designate a receiving station and, therefore, no need to uplink such information to the user spacecraft.

a. COS With 3 × 3 Stations. The clustered optical subnet to be discussed in detail consists of nine stations located in three clusters of three stations (COS 3 × 3); the clusters are approximately 120 deg apart in longitude (approximately 14,000 km). This configuration provides 96 percent weather availability since the stations are located within a cluster at distances no more than a few hundred kilometers apart.

Ideal coverage curves to model a COS 3 × 3, with the clusters located 120 deg apart in longitude, are seen as a subset of the curves for the LDOS configuration with six stations, which is shown in Fig. 12. (Consider curves 1(a), 3, 5, and 1(b) only.) The assumptions about the sites are the same as those described for the LDOS with six stations (see above); however, it is assumed that only one site in the cluster is receiving telemetry. The weather availability of this configuration is 96 percent, and the telemetry line is at $\zeta = 60$-deg zenith angle, which is where the handing over to the following cluster takes place.

The geographical cluster locations chosen for the COS 3 × 3 are shown in Fig. 14. Table 5(a) provides a list of the specific geographical sites and their weather statistics. Like the sites chosen for the LDOS subnet, each COS 3 × 3 site has cloud-free days at least 66 percent of the time. In this configuration, each cluster is dedicated to a single user pass, resulting in a 96 percent probability that at least one optical station will have a clear LOS to the user.

Figure 15 shows the coverage curves for the COS 3 × 3 stations when data on one of the three actual geographical sites in each cluster are used for a Pluto mission in 2015. The actual sites used to obtain the coverage curves are TMF in California, Siding Spring Mt. in Australia, and Calar Alto in Spain. The site-specific information used to obtain these curves includes altitude, longitude, and latitude, as well as Pluto's trajectory across the sky. Note that Pluto does not pass through the zenith for any of the sites.

Like the LDOS configuration discussed above, the characteristic performance of the optical channel at approximately 70 deg off zenith (hand-over) is the determining factor for telemetry performance. The telemetry curve for the Pluto mission is placed at −6.2 dB, compared to −4.7 dB for the ideal case. However, even with this change, two gaps exist in the LOS coverage, totaling about 4 hours per day. The LOS coverage provided by the COS 3 × 3 for a Pluto mission in 2015 is about 79 percent. As is the case with the LDOS concept, each optical terminal has about 20 minutes to acquire, track, and lock onto the incoming optical beam. The total network availability has not changed, since each cluster contains three sites in independent weather cells.

Although this configuration provides the same telemetry rate as the LDOS network with six stations and better weather availability, the gaps in coverage and the significantly larger number of stations required for the clustered concept are distinct disadvantages.

b. COS With 3 × 4 Stations. A total of 12 optical stations will be necessary in this subnet configuration (COS 3 × 4). The distance between clusters will be roughly 90 deg in longitude (approximately 10,000 km).

Table 5(b) shows a list of probable geographical sites for COS 3 × 4. Each cluster (numbered 1 to 4) contains three optical station sites to satisfy the ground rules for the COS concept discussed above.

3. Network Availability. Weather-related availabilities for the idealized network configurations are shown in the second column of Table 6. The probabilities have been calculated using the model described above, with $q = 0.34$ for each individual site. Additionally, the acceptable zenith angle loss, or the telemetry line, used to calculate availabilities for the ideal LDOS networks is consistent with a 60-deg zenith angle, and the link calculations shown in Sections IV.E and IV.F below are based on this assumption. The telemetry line, however, can be made consistent with a 75-deg zenith angle to increase network availability to 92, 95, and 96 percent for an LDOS with 6, 7, or 8 stations, respectively. The trade-offs to identify optimum position for the telemetry line were not performed.

For an actual LDOS with six stations for the Pluto mission, a telemetry line at a 70-deg zenith angle was used

to calculate the network availability and the data rates shown in Section IV.F. The weather availability for the specific Pluto mission for an LDOS with six stations and for a COS with three clusters of three stations each is shown in the third column in Table 6.

4. Network Coverage. Table 7 shows that the LOS coverage for all idealized optical subnet configurations considered here is 100 percent. The coverage numbers for the actual geographical sites chosen for an LDOS with six stations and a COS 3 × 3 for a Pluto mission in 2015 are shown in the third column of the same table. Note that the coverage for the COS 3 × 3 for this specific case drops to 79 percent. The LOS coverage for COS 3 × 4 and LDOS with seven or eight stations with actual sites considered was not calculated but is expected to be 100 percent.

E. Link Calculations

Link analysis for a 30-AU Pluto mission at night was performed using OPTI 4.0, a software package developed in-house at JPL (see Appendix A).

1. Operational Considerations. The operational parameters used to estimate the telemetry capacity in this study are shown in Table 8. Details on other parameters used in the communication link budget are shown in Appendix A.

The modulation format used with the OPTI software was PPM. The alphabet size, as shown in Table 8, is 256.

A nominal raw link bit error rate (BER) of 0.013 was used. This was reduced to 10^{-5} by applying 7/8 Reed–Solomon coding. The 7/8 correction was applied to the data rate calculated by OPTI.

F. Telemetry

The telemetry return capability was used as the primary measure of the subnet performance. The benchmark established in the study for telemetry was 240 kb/sec for a future 70-m Ka-band (32 GHz) receiver, averaged over a 24-hour period. The user spacecraft antenna for this benchmark is 5 m in diameter.

The following assumptions and procedures were followed to calculate telemetry return capability for optical communications:

(1) The user spacecraft employs a transmitter proposed by TRW for its DSRSS study.[7] It is based on a 0.75-m telescope and a 7-W laser operating at 532-nm wavelength. See Appendix A for a list of transmitter parameters used.

(2) The optical terminal is based on a 10-m telescope. See Appendix A for a list of receiver parameters.

(3) Data rates for night and day were calculated separately. For the daytime calculation, an average data rate was computed over a number of daytime sky-radiance values.

(4) Data rates were computed for an ideal optical subnet and a realistic network for a 30-AU mission to Pluto in 2015.

(5) Data rates were computed for a conventional filter with a spectral bandwidth of 0.1 nm and for an atomic resonance filter with a spectral bandwidth of 0.001 nm.

(6) Daytime and nighttime data rates were averaged over a period of 24 hours for both optical filters, and telemetry improvement over the baseline was calculated.

1. Telemetry for the 30-AU Pluto Mission. Table 9 summarizes the data rates, which have been corrected for coding as discussed below, expected for an optical communications link between a 0.75-m user spacecraft transmitter at 30 AU and a 10-m ground station. Data rates using an atomic resonance filter (ARF) as well as a conventional filter were calculated for both an ideal configuration and a specific mission to Pluto in 2015. The acceptable zenith angle losses through the atmosphere for the ideal case and the actual Pluto mission were −4.7 dB (consistent with a 60-deg zenith angle) and −6.2 dB (consistent with a 70-deg zenith angle) respectively. The daytime data rate was obtained by averaging data rates calculated for six representative day-sky radiances between 10 and 180 deg solar elongation.

The data rates were first calculated using OPTI 4.0 for a 0.013 BER without coding. This raw data rate was then multiplied by 0.877 to obtain a 7/8 Reed–Solomon (R–S) coded data rate with a 10^{-5} BER for PPM modulation with an alphabet size of $M = 256$.[8] The dB gain, shown in parentheses with each data rate, was calculated over the agreed baseline telemetry rate of 240 kb/sec. Note that the data rates shown in Table 9 were not corrected for weather availability or the LOS coverage.

[7] TRW briefing, "Deep Space Relay Satellite System Study," Quarterly Progress Review, presented to JPL on February 25, 1993.

[8] W. Marshall, "Using the link analysis program with R–S encoded links," JPL Interoffice Memorandum 331-86.6-202 (internal document), Jet Propulsion Laboratory, Pasadena, California, August 1, 1986.

Table 9 shows that a ground-based optical subnet can provide very high data rates. For the Pluto mission at 30 AU, the telemetry rate can be as high as 1716 kb/sec, about 8.5 dB higher than the baseline rate of 240 kb/sec. Daytime data rates are lower, as expected, but still provide improvement over the baseline performance.

The telemetry rate can be further improved by employing 12- to 15-m receiver apertures. The technology for photon buckets up to 15 m in size is within reach with low technical risk. Use of a larger aperture, for a given data rate, is expected to have a favorable impact on the user-spacecraft design. It will usually mean a user-spacecraft optical terminal with smaller mass, size, and power consumption.

V. Conclusion

Several alternative optical subnet configurations were considered in this article. It is seen that an LDOS with six stations can provide nearly full LOS coverage of the ecliptic and 81 percent weather availability. If higher availabilities are needed, an LDOS with seven or eight stations can be used.

COS 3 × 3 under realistic conditions fails to provide full coverage (it provides approximately 79 percent). If the clustered concept for the optical subnet is desirable, a COS 3 × 4 with 12 ground stations will be required to provide full coverage, at least for the Pluto mission in 2015. The availability of both COS configurations is expected to be 96 percent. The COS configuration imposes an additional requirement over the LDOS configuration for locating appropriate specific sites. The clusters must be about 90 deg apart in longitude for COS 3 × 4, and intracluster station distances must be at least 150 km to ensure decorrelation of weather statistics. This may make it more difficult to find three specific sites within a given cluster when other requirements such as high altitude and reasonable accessibility are included.

A linearly dispersed optical subnet with six to eight stations is recommended, since it accomplishes the task with fewer ground stations than any other configuration considered here.

References

[1] K. Shaik, "Progress on ten-meter optical receiver telescope," *SPIE*, vol. 1635, edited by D. L. Begley and B. D. Seery, pp. 109–117, 1992.

[2] K. Shaik, "A Preliminary Weather Model for Optical Communications Through the Atmosphere," *The Telecommunications and Data Acquisition Progress Report 42-95, vol. July–September 1988*, pp. 212–218, November 15, 1988.

[3] K. Shaik and J. Churnside, "Laser Communication Through the Atmosphere," *Proceedings of the Twelfth NASA Propagation Experimenters Meeting (Napex XII)*, Syracuse, New York, pp. 126–131, June 9–10, 1988.

[4] J. Nelson, T. Mast, and S. Faber, "The Design of the Keck Observatory and Telescope," Keck Observatory Report No. 90, Keck Observatory, Mauna Kea, Hawaii, pp. 2–11, 1985.

[5] D. P. Wylie and W. P. Menzel, "Cloud cover statistics using VAS," *Nonlinear Optical Beam Manipulation, Beam Combining, and Atmospheric Propagation, Proceedings of the Meeting*, Los Angeles, California, January 11–14, 1988, pp. 253–259, 1988.

[6] *Greenhouse Effect Detection Experiment (GEDEX), 1992 Update*, CD-ROM, World Data Center for Rockets and Satellites, Code 902.2 DAAC, NASA Goddard Space Flight Center, Greenbelt, Maryland, 1992.

[7] The Association of Universities for Research in Astronomy (AURA), *The NOAO 8 m Telescopes* (now called Gemini 8-m telescopes), proposal to the National Science Foundation, AURA, Washington, DC, 1989.

Table 1. Telescope description.

Parameter	Value
System focal length, m	77.5
System focal ratio	7.75
System scale at Cassegrain focus, μrad/mm	12.9
System blur diameter, μrad	$\leq$100
System FOV at Cassegrain focus, mrad	2.0
Primary mirror size, m	10
Primary radius of curvature, m	−10.0
Primary focal ratio	0.5
Primary aspheric deformation	−1.0009
Primary to secondary distance, m	−4.5
Secondary mirror size, m	1.0
Secondary radius of curvature, m	−1.069
Secondary aspheric deformation	−1.3062
Secondary to Cassegrain focus distance, m	7.75

Table 2. Pointing, tracking, and slewing capability.

Parameter	Value
Coarse blind pointing, mrad	0.2
Fine pointing, mrad	0.01
Tracking rate, both axes, deg/sec	0.005
Slew rate for both axes, deg/sec	1.0
Acceleration/deceleration for both axes, deg/sec^2	3.0

Table 3. Transmitter parameters.

Transmitter parameter	Value
Average power, W	7
Wavelength, nm	532
Aperture size, m	0.75
Obscuration, m	0.0
Optics efficiency	0.8
Pointing bias error, μrad	0.1
RMS pointing jitter, μrad	0.1

Table 4(a). Linearly dispersed optical subnet with six ground optical stations.

Location	Altitude, km	Longitude, deg	Latitude, deg	Time zone	Cloud-free days/weather	Preexisting facilities and infrastructure
Southwest United States Table Mountain Facility, Calif.	2.3	118 W	34 N	−8	66%/arid[a]	Yes
Hawaii, United States Mauna Kea	4.2	155 W	20 N	−10	>69%/dry [7]	Yes
Australia Siding Spring Mountain	1.1	149 E	31 S	+10	67%/dry	Yes
Pakistan Ziarat	2.0	68 E	30 N	+5	69%/arid	Information NA
Spain/Northwest Africa Calar Alto, Spain	2.2	2 W	37 N	−1	67%/arid	Yes
South America Cerro Pachan, Chile	2.7	71 W	30 S	−4	77%/arid [7]	Yes

[a] ISCCP satellite data, obtained from [6].

Table 4(b). Linearly dispersed optical subnet with seven locations.

Location	Altitude, km	Longitude, deg	Latitude, deg	Time zone	Cloud-free days/weather	Preexisting facilities and infrastructure
Southwest United States Table Mountain Facility, Calif.	2.3	118 W	34 N	−8	66%/arid[a]	Yes
Hawaii, United States Mauna Kea	4.2	155 W	20 N	−10	>69%/dry [7]	Yes
Australia Siding Spring Mountain	1.1	149 E	31 S	+10	67%/dry	Yes
Nepal/South India	NA	NA	NA	+6	NA	Information NA
Saudi Arabia Jabal Ibrahim	2.6	41 E	21 N	+3	NA	Information NA
Spain/Northwest Africa Calar Alto, Spain	2.2	2 W	37 N	−1	67%/arid	Yes
South America Cerro Pachan, Chile	2.7	71 W	30 S	−4	77%/arid [7]	Yes

[a] ISCCP satellite data, obtained from [6].

Table 4(c). Linearly dispersed optical subnet with eight locations. Each of the eight listed locations will have a ground optical receiving station.

Location	Altitude, km	Longitude, deg	Latitude, deg	Time zone	Cloud-free days/weather	Preexisting facilities and infrastructure
Southwest United States						
Table Mountain Facility, Calif.	2.3	118 W	34 N	−8	66%/arid[a]	Yes
Hawaii, United States						
Mauna Kea	4.2	155 W	20 N	−10	>69%/dry [7]	Yes
Australia						
Siding Spring Mountain	1.1	149 E	31 S	+10	67%/dry	Yes
Australia						
Mt. Bruce	1.2	118 E	23 S	+8	NA/dry	Information NA
Pakistan						
Ziarat	2.0	68 E	30 N	+5	69%/arid	Information NA
Saudi Arabia						
Jabal Ibrahim	2.6	41 E	21 N	+3	NA	Information NA
Spain/Northwest Africa						
Calar Alto, Spain	2.2	2 W	37 N	−1	67%/arid	Yes
South America						
Cerro Pachan, Chile	2.7	71 W	30 S	−4	77%/arid [7]	Yes

[a] ISCCP satellite data, obtained from [6].

Table 5(a). Clustered optical subnet locations. The network consists of three ground optical receiving stations in each of the three locations.

Location	Altitude, km	Longitude, deg	Latitude, deg	Time zone	Cloud-free days/weather	Preexisting facilities and infrastructure
Southwest United States						
Table Mountain Facility, Calif.	2.3	118 W	34 N	−8	66%/dry[a]	Yes
Mt. Lemmon, Arizona	2.1	111 W	31 N	−7	>60%/dry [7]	Yes
Sacramento Peak, New Mexico	3.0	106 W	35 N	−7	>60%/dry [7]	Yes
Australia						
Mt. Bruce	1.2	118 E	23 S	+8	NA	Information NA
Mt. Round	1.6	153 E	30 S	+10	NA	Information NA
Siding Spring Mountain	1.1	149 E	31 S	+10	67%/dry	Yes
Spain/Northwest Africa						
Arin Ayachi, Morocco	3.7	5 W	33 N	0	NA	Information NA
Tahat, Algeria	2.9	5 W	22 N	−1	NA	Information NA
Calar Alto, Spain	2.2	2 W	37 N	−1	67%/dry[a]	Yes

[a] ISCCP satellite data, obtained from [6].

Table 5(b). Clustered optical subnet locations. The network consists of three ground optical receiving stations in each of the four locations.

Location	Altitude, km	Longitude, deg	Latitude, deg	Time zone	Cloud-free days/weather	Preexisting facilities and infrastructure
Southwest United States						
Table Mountain Facility, Calif.	2.3	118 W	34 N	−8	66%/dry[a]	Yes
Mt. Lemmon, Arizona	2.1	111 W	31 N	−7	>60%/dry [7]	Yes
Sacramento Peak, New Mexico	3.0	106 W	35 N	−7	>60%/dry [7]	Yes
Australia						
Mt. Bruce	1.2	118 E	23 S	+8	NA	Information NA
Mt. Round	1.6	153 E	30 S	+10	NA	Information NA
Siding Spring Mountain	1.1	149 E	31 S	+10	67%/dry[a]	Yes
Pakistan						
Ziarat	2.0	68 E	30 N	+5	69%/arid	Information NA
Site not determined	—	—	—	—	—	—
Site not determined	—	—	—	—	—	—
Spain/Northwest Africa						
Arin Ayachi, Morocco	3.7	5 W	33 N	0	NA	Information NA
Tahat, Algeria	2.9	5 W	22 N	−1	NA	Information NA
Calar Alto, Spain	2.2	2 W	37 N	−1	67%/dry[a]	Yes

[a] ISCCP satellite data, obtained from [6].

Table 6. Network availability.

Network	Availability with ideal sites, percent	Availability with actual sites, percent
COS 3x3	96	96
COS 3x4	96	96
LDOS: six stations	88	81
LDOS: seven stations	91	—
LDOS: eight stations	94	—

Table 7. Network coverage.

Network	Coverage with ideal sites, percent	Coverage with actual sites, percent
COS 3x3	100	79
COS 3x4	100	—
LDOS: six stations	100	95
LDOS: seven stations	100	—
LDOS: eight stations	100	—

Table 8. Operational parameters for link calculations.

Parameter	Value
PPM alphabet size	256
Link distance, AU	30
Raw bit-error rate	0.013
Slot width, nsec	10

Table 9. Nighttime, daytime average, and day/night average data rates (kb/sec) for a 10-m ground receiver, and average gain (dB) over baseline telemetry for the receiver with an atomic resonance filter (ARF) and with a conventional filter. The user spacecraft transmitter is at a distance of 30 AU and has a telescope 0.75 m in size. The data rates were not corrected for weather availability and LOS coverage.

Period	Ideal LDOS with six stations				Actual LDOS with six stations for a Pluto mission in 2015			
	ARF filter[a]		Conventional filter[b]		ARF filter[a]		Conventional filter[b]	
	kb/sec	dB gain[c]	kb/sec	dB gain[c]	kb/sec	dB gain[c]	kb/sec	dB gain[c]
Nighttime	1716	8.5	1716	8.5	1215	7.0	1215	7.0
Daytime average[d]	1056	6.4	377	2.0	774	5.1	298	0.94
Day/night average	1386	7.6	1047	6.4	994	6.2	757	5.0

[a] The ARF filter has a bandwidth of 0.001 nm.
[b] The conventional filter has a bandwidth of 0.1 nm.
[c] The dB gain is calculated over a baseline telemetry rate of 240 kb/sec.
[d] The daytime average is obtained by averaging data rates calculated for six day-sky radiances between 10- and 180-deg solar elongation.

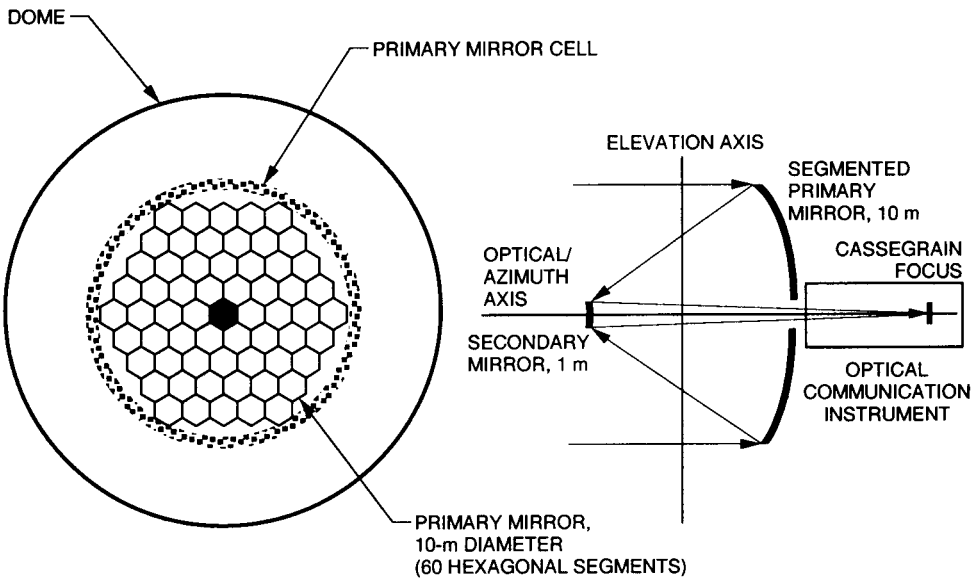

Fig. 1. Conceptual diagram of the 10-m telescope for the ground optical terminal (not drawn to scale). Primary diameter = 10 m; FOV at Cassegrain focus = 2.0 mrad; coarse pointing accuracy = 0.2 mrad; FOV at detector = 0.1 mrad; fine pointing accuracy = 0.01 mrad; and the blur diameter at focus $\leq$ 0.1 mrad.

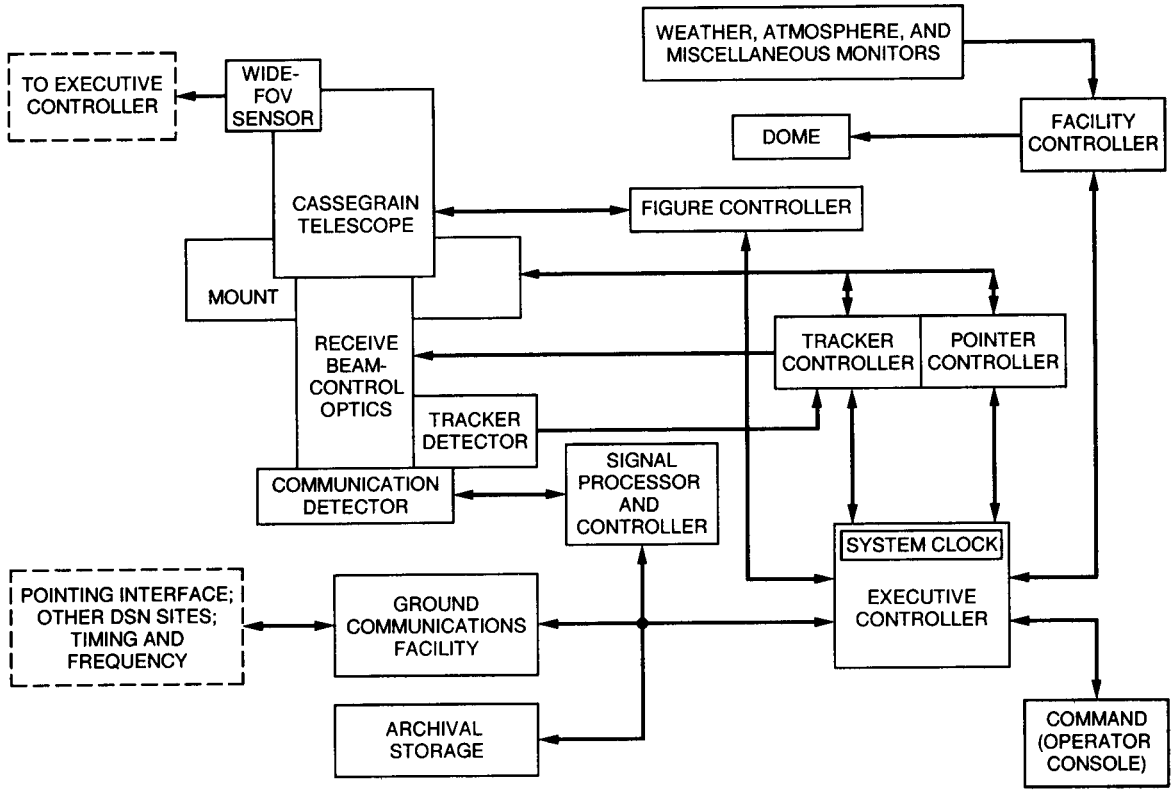

Fig. 2. Ground optical station block diagram.

I. OPTICAL TERMINAL:
   A. TELESCOPE AND OPTICS
   B. RECEIVER SUBSYSTEM
   C. ACQUISITION POINTING AND TRACKING
   D. ENVIRONMENTAL HOUSING

II. DATA PROCESSING:
   A. TIMING AND FREQUENCY
   B. SIGNAL PROCESSING
   C. CONTROL AND MONITOR
   D. GROUND COMMUNICATIONS
   E. ARCHIVAL STORAGE
   F. SIMULATION, TEST AND TRAINING

III. FACILITIES:
   A. BUILDINGS
   B. ROADS/WATER/SEWAGE
   C. POWER/GROUND SUBSYSTEM/UNINTERRUPTIBLE POWER SUPPLY
   D. HEAT, VENTILATION, AND AIR CONDITIONING/ FIRE SUPPRESSION/SECURITY
   E. WEATHER SUBSYSTEM
   F. LEASED TELECOMMUNICATIONS SERVICES

IV. LOGISTICS:
   A. ON-SITE EQUIPMENT SPARES
   B. DIAGNOSTICS, TOOLING, AND TEST EQUIPMENT
   C. TRANSPORTATION

V. OPERATIONS:
   A. WORKFORCE
   B. ADMINISTRATION/MATERIAL/TRAINING

Fig. 3. Optical station system breakdown.

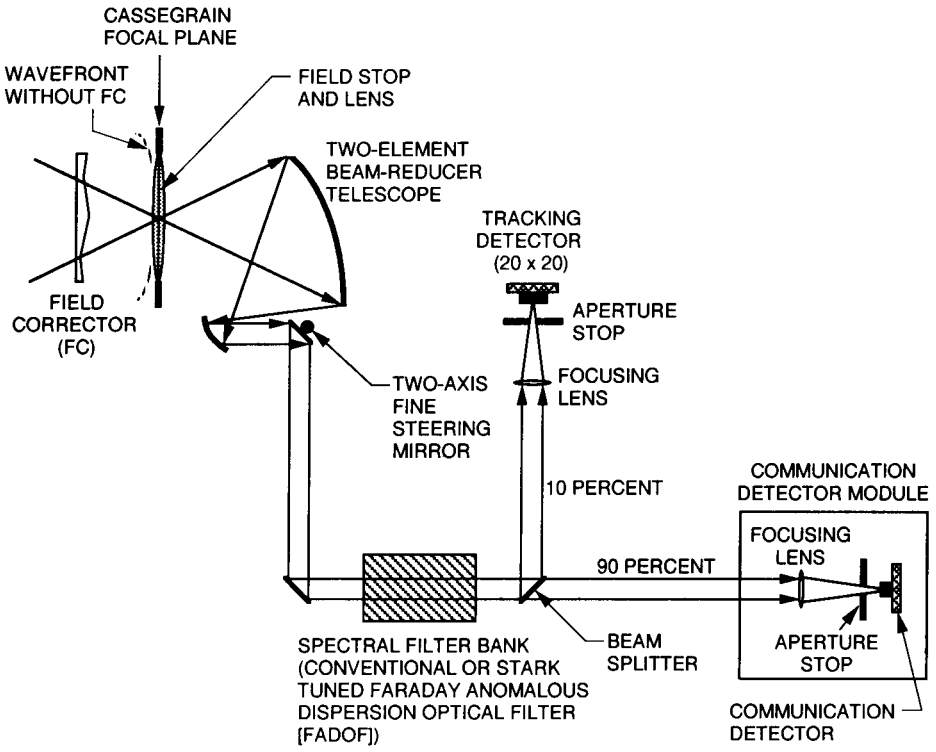

Fig. 4. Conceptual diagram for an optical communications instrument (not drawn to scale).

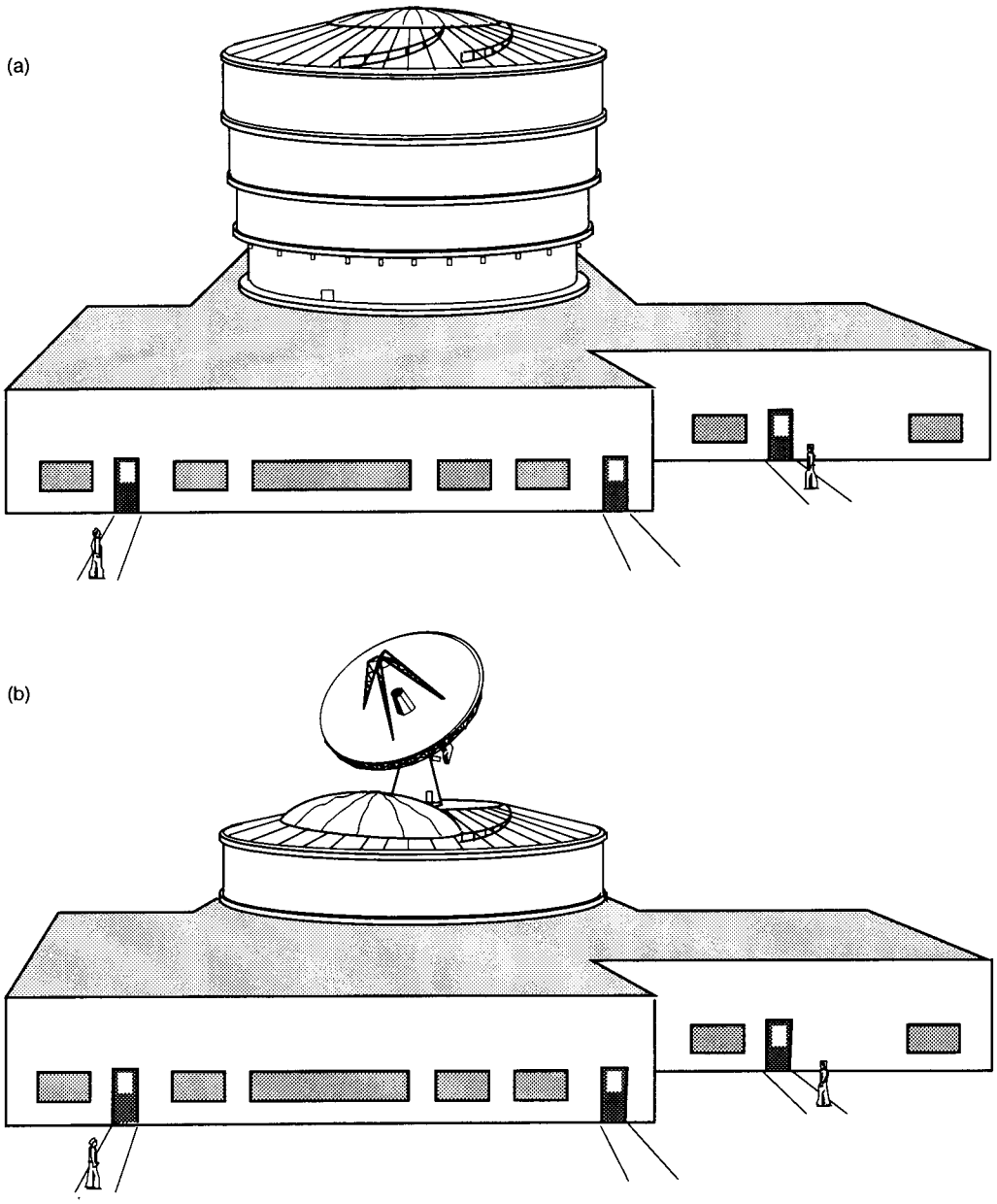

Fig. 5. Typical protective dome for the receiver telescope: (a) closed and (b) open (not drawn to scale).

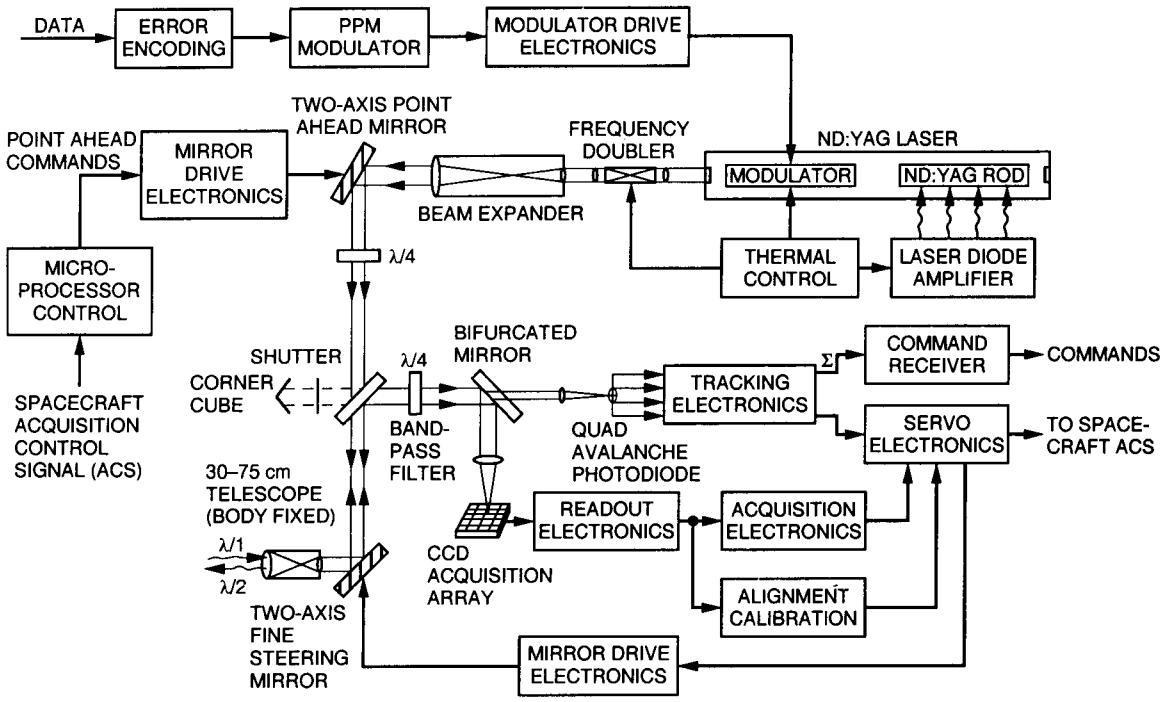

Fig. 6. Block diagram for the user terminal. (The terminal is based on TRW's conceptual design of a user terminal, done as part of a DSRSS study. The conceptual design was presented to JPL on February 25, 1993, as part of a quarterly progress review on the study.)

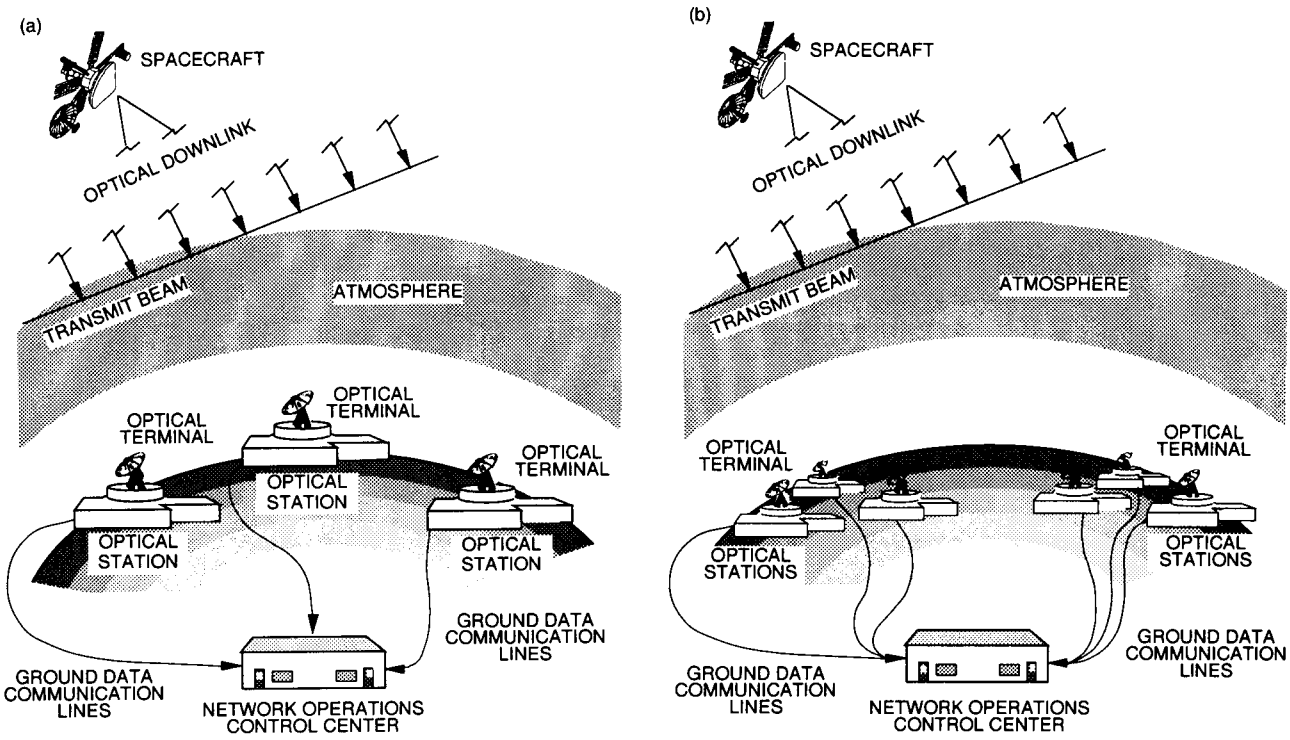

Fig. 7. Network geometry (not drawn to scale): (a) LDOS and (b) COS.

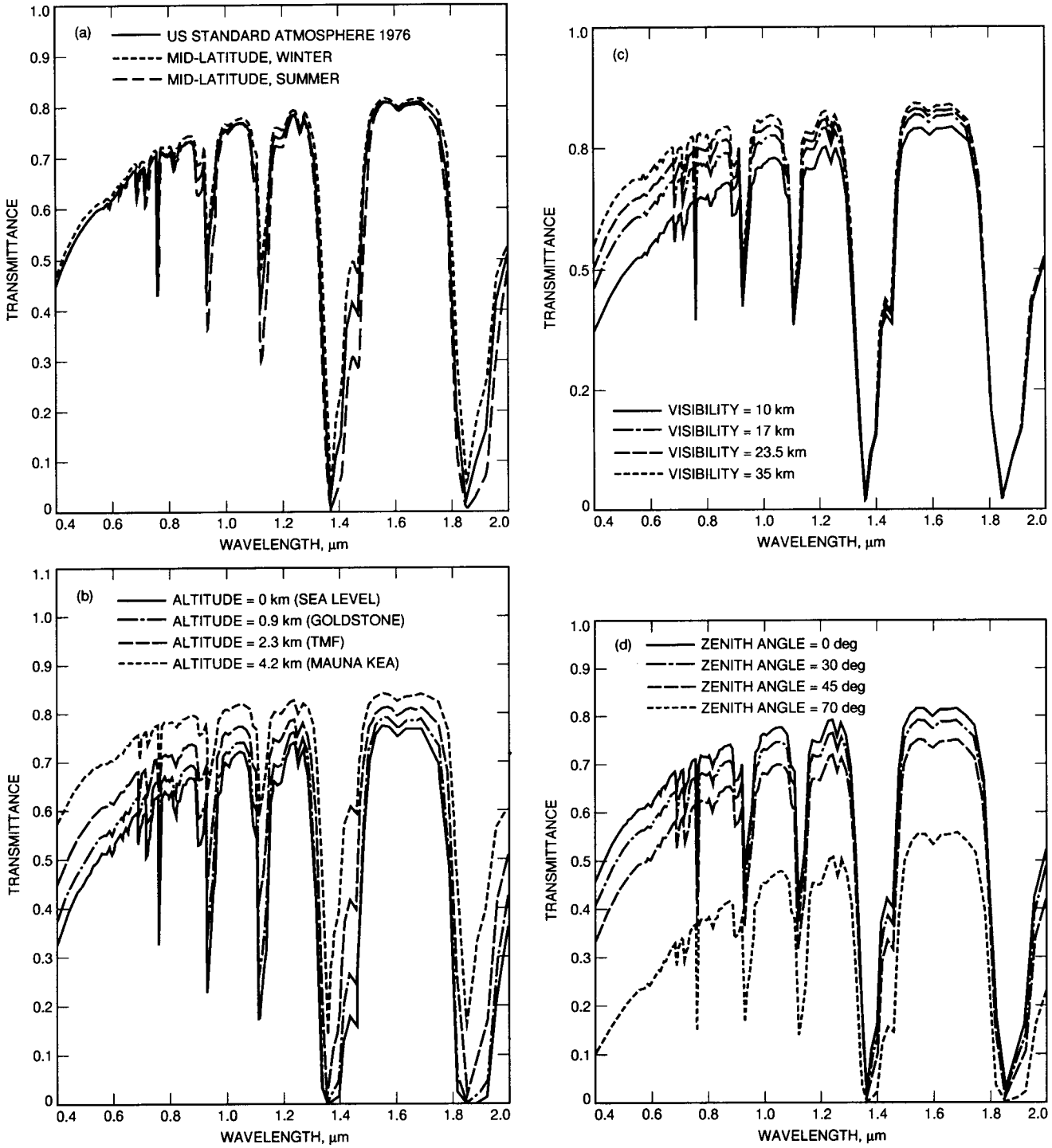

Fig. 8. Spectral transmittance data. All four diagrams assume high cirrus clouds. (a) Spectral transmittance over visible and near-infrared wavelengths for three LOWTRAN atmospheric models. (The diagram assumes a 2.3-km altitude, a 17-km meteorological range [clear], and a zenith path through the atmosphere). (b) Spectral transmittance for selected altitudes over visible and near-infrared wavelengths. (The diagram assumes the use of the U.S. Standard Atmosphere 1976 model, a 17-km meteorological range [clear], and a zenith path through the atmosphere). (c) Spectral transmittance for selected meteorological ranges (visibilities) over visible and near-infrared wavelengths. (The diagram assumes the U.S. Standard Atmosphere 1976 model, a 2.3-km altitude, and a zenith path through the atmosphere.) (d) Spectral transmittance for selected zenith angles over visible and near-infrared wavelengths. (The diagram assumes the U.S. Standard Atmosphere 1976 model, a 2.3-km altitude, a 17-km meteorological range [clear], and a slant path through the atmosphere).

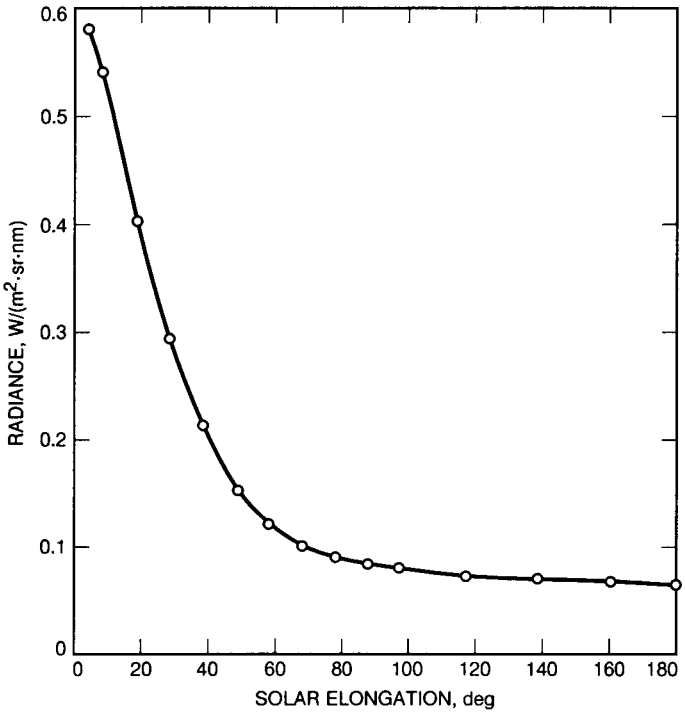

Fig. 9. Daytime sky radiance as a function of solar elongation (Sun–Earth–probe angle).

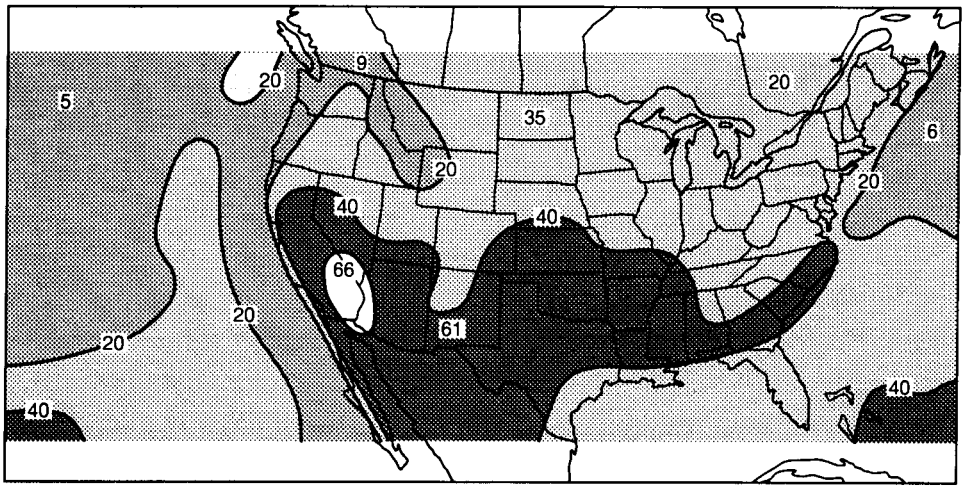

Fig. 10. Contour diagram obtained from two years of GOES satellite data; the diagram shows the probability of clear skies over the United States.

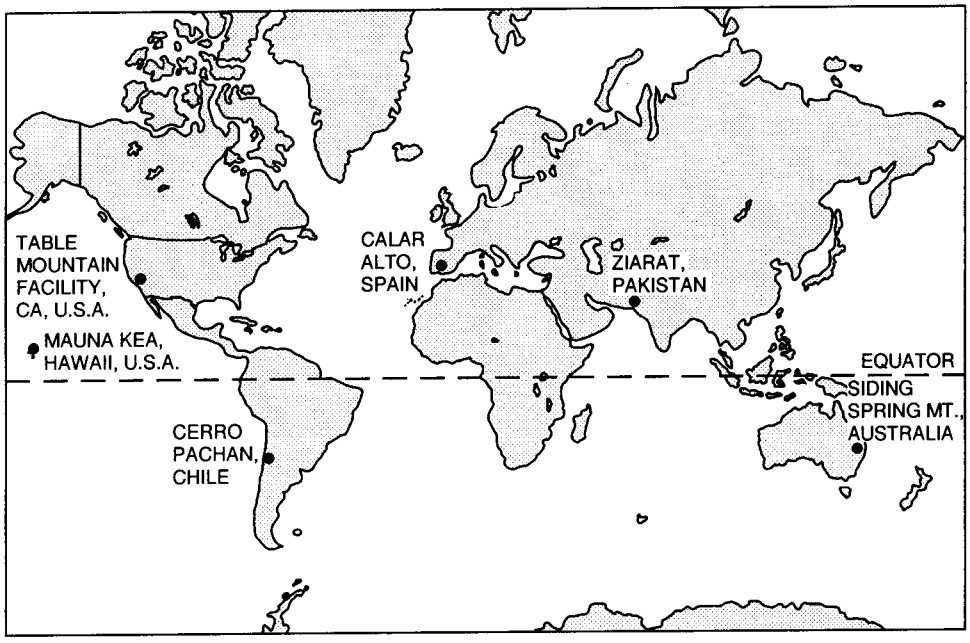

Fig. 11. Geographical sites for an LDOS with six stations.

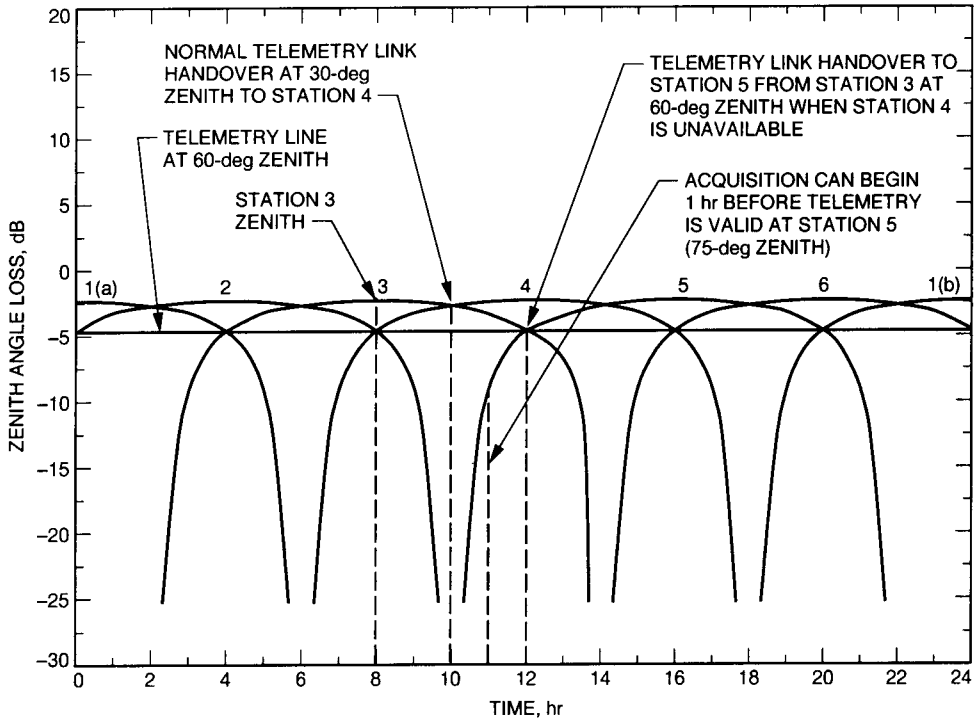

Fig. 12. Ideal-coverage curves over one day for an LDOS subnet with six stations 60 deg apart in longitude in an equatorial belt.

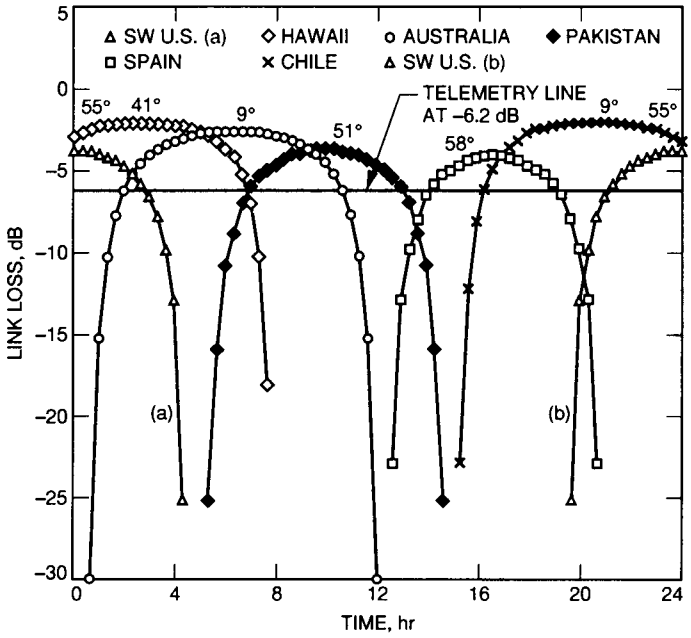

Fig. 13. Coverage curves for six actual sites for a Pluto link in 2015. Zenith angles at local meridian for Pluto in 2015 are shown at the top of each curve. The sites used are shown in Table 3. The coverage curve for the southwestern United States is shown in two halves: SW U.S. (a) and SW U.S. (b).

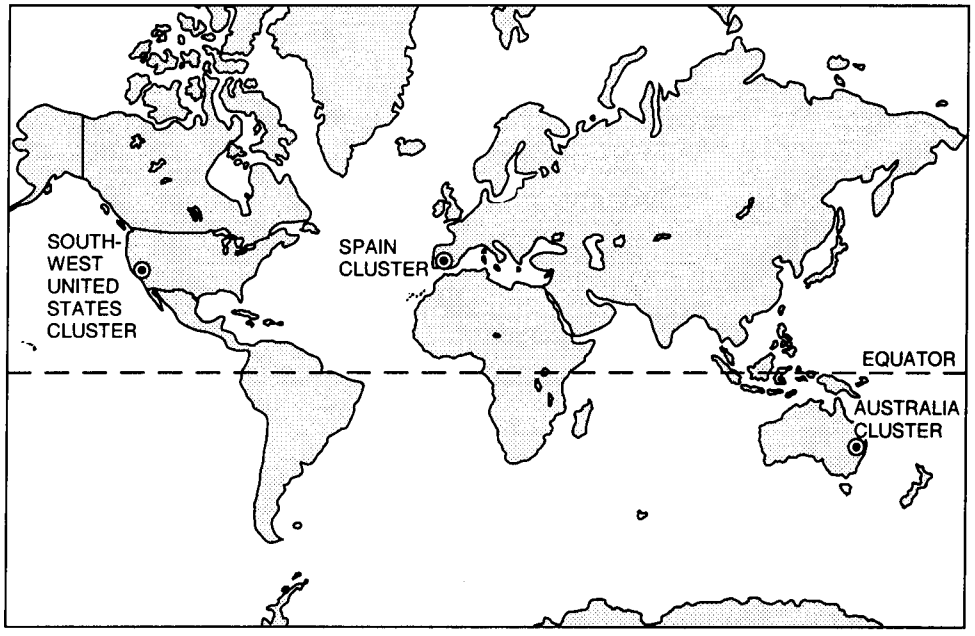

Fig. 14. Geographical sites for the COS 3 × 3 subnet.

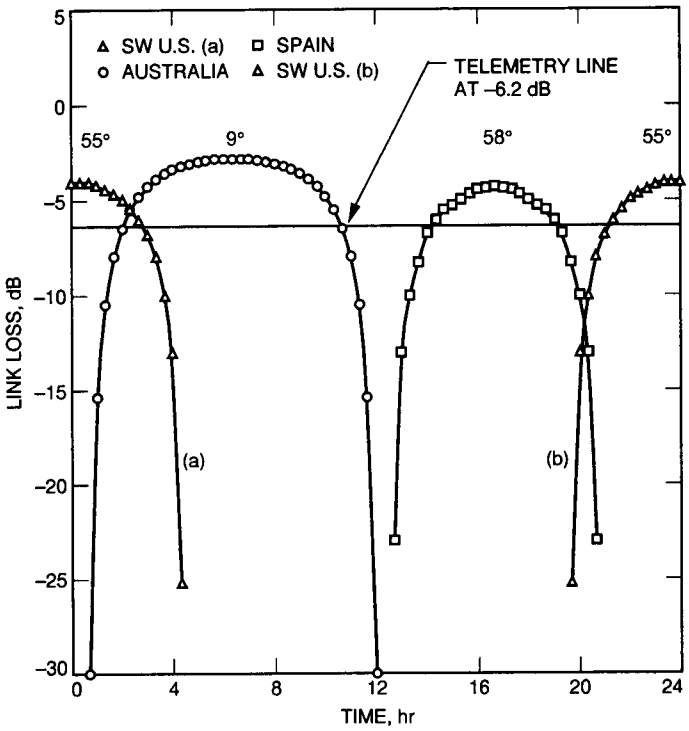

Fig. 15. Coverage curves for a COS 3 × 3 subnet with nine stations for a Pluto mission in 2015. Zenith angles at local meridian for Pluto in 2015 are shown at the top of each curve. The sites used to calculate the coverage curves are TMF in California, Siding Spring Mt. in Australia, and Calar Alto in Spain (see Table 3). The coverage curve for the southwestern United States is shown in two halves: SW U.S. (a) and SW U.S. (b).

Appendix A

OPTI Sample Output

OPTICAL COMMUNICATIONS LINK ANALYSIS PROGRAM
VERSION 4.02
GBATS, 30 AU, nighttime, 70° zenith angle, ARF spectral filter
PPM Direct Detection PMT detector

The transmitter parameters are (user spacecraft):

Transmitter average power (watts)	= 7.0000
Wavelength of laser light (micrometers)	= 0.53200
Transmitter antenna diameter (meters)	= 0.75000
Transmitter obscuration diameter (meters)	= 0.00000
Transmitter optics efficiency	= 0.80000
Transmitter pointing bias error (microrad.)	= 0.10000
Transmitter rms pointing jitter (microrad.)	= 0.10000
Modulation extinction ratio	= 0.10000E+06

The receiver parameters are (ground station):

Diameter of receiver aperture (meters)	= 10.000
Obscuration diameter of receiver (meters)	= 3.0000
Receiver optics efficiency	= 0.70000
Detector quantum efficiency	= 0.21000
Narrowband filter transmission factor	= 0.60000
Filter spectral bandwidth (angstroms)	= 0.10000E-01
Detector dia. field of view (microrad.)	= 100.00

The operational parameters are:

Alphabet size (M = ?)	= 256.00
Data rate (kb/s)	= 1387.8
Link distance (A.U.)	= 30.000
Required link bit error rate	= 0.13000E-01
Atmospheric transmission factor	= 0.24000
Dead time (microseconds)	= 3.2046
Slot width (nanoseconds)	= 10.000

Noise sources

Pluto	RCVR to source distance (AU)	= 30.000

Additional noise sources

nightsky	radiance(W/M**2/SR/A)	= .50000E-08

		Factor	dB
Laser output power (watts)		7.00	38.5 dBm
Min Req'd peak power (watts)	= .40E+04		
Transmitter antenna gain		0.160E+14	132.0
Antenna dia. (meters)	= 0.750		
Obscuration dia.(meters)	= 0.000		
Beam width (microrad)	= 1.121		
Transmitter optics efficiency		0.800	-1.0
Transmitter pointing efficiency		0.893	-0.5
Bias error (microrad)	= 0.100		
RMS jitter (microrad)	= 0.100		
Space loss (30.00 AU)		0.890E-40	-400.5
Receiver antenna gain		0.446E+16	156.5
Antenna dia. (meters)	= 10.000		
Obscuration dia. (meters)	= 3.000		
Field of view (microrad.)	= 100.000		
Receiver optics efficiency		0.700	-1.5
Narrowband filter transmission		0.600	-2.2
Bandwidth (angstroms)	= 0.010		
Detector Quantum efficiency		0.210	-6.8
Atmospheric transmission factor		0.240	-6.2
Received signal power (watts)		0.228E-11	-86.4 dBm
Recv'd background power (watts)	= 0.323E-17		
Photons/joule		0.268E+19	154.3 dB/mJ
Detected signal PE/second		0.255E+07	64.1 dBHz
Symbol time (seconds)		0.290E-05	-55.4 dB/Hz
Detected signal PE/symbol		7.36	8.7
Required signal PE/symbol		3.69	5.7
Detected background PE/slot	= 0.736E-04		
Margin		2.00	3.0

Appendix B
Site-Selection Guidelines and Procedures

I. Selection Guidelines

The following guidelines were used to identify probable sites for the Earth-based optical communication terminals:

(1) Locations as close to the equator as possible.

(2) High altitudes, preferably mountaintops.

(3) Good astronomical seeing.

(4) A large number of cloud-free days per year.

(5) Accessible locations with existing infrastructure, if possible.

II. Selection Procedure

To start, large geographical regions with an appropriate distance in longitude between them for the network configuration under consideration, and as close to the equator as possible, were identified on a map. A detailed literature search was then performed to locate sites at high altitudes in each region, thus generating a large list of likely station sites. Sites with good astronomical seeing, a large number of cloud-free days, and a preexisting infrastructure were favored. Inaccessible sites with wet weather were dropped from consideration when better alternates were available.

III. List of Additional Possible Sites

Table B-1 provides a list of geographical sites in addition to those already listed in the main text of this article. Each possible site in this table, and in the site tables shown elsewhere in this article, is followed by its altitude, longitude, latitude, and the time zone. The next column provides information on the number of cloud-free days and the weather of the site. The cloud-cover data on most sites were obtained from the International Satellite Cloud Climatology Project (ISCCP) as managed by the NASA Climate Data System (NCDS) and are available on CD-ROM [6]. The data provide monthly averages over an eight-year period ending in December 1990, for the entire globe, with a resolution of 250 km.[1] Data on other sites, like Mauna Kea in Hawaii, were obtained in situ for astronomical purposes. The last column indicates if there is a preexisting infrastructure at the site.

The lists of actual sites presented in this article should be treated as tentative and preliminary.

---

[1] K. Shaik and D. Wonica, "Cloud cover data for GBATS," JPL Interoffice Memorandum 331.6-93-098 (internal document), Jet Propulsion Laboratory, Pasadena, California, May 6, 1993.

Table B-1. Additional sites of interest for an optical communications network.

Location	Altitude, km	Longitude, deg	Latitude, deg	Time zone	Cloud-free days/weather	Preexisting facilities and infrastructure
Roque de los Muchachos Observatory, Canary Islands, Spain	NA	16 W	29 N	−2	NA/dry	Yes
Fuente Nueva, La Palma Canary Islands, Spain	NA	16 W	29 N	−2	NA/dry	Yes
Jabal Toukal, Morocco	4.1	8 W	31 N	0	NA/dry	Information NA
Mulhecen, Spain	3.4	3 W	37 N	−1	67%/dry[a]	Information NA
Inaña, Tenerife, Canary Islands, Spain	NA	16 W	29 N	−2	NA/dry	Yes
Cerro Tololo, Chile	2.2	71 W	30 S	−4	77%/arid [7]	Yes
Llano del Hato, Venezuela	3.6	71 W	9 N	−4	NA/dry	Yes
Mt. Ziel, Australia	1.5	133 E	23 S	10	NA/dry	Information NA
Freeling Heights, Australia	1.1	139 E	30 S	10	NA/dry[b]	Information NA

[a] ISCCP satellite data, obtained from [6].

[b] A. Rogers, personal communication, Australian National University, Mount Stromolo and Siding Spring Observatories, Canberra, Australia, June 1993.